

Lecture 5

Linear and non-linear tearing Modes

J. P. Graves

5. Linear and non-linear Tearing Modes

Types of resistive modes instabilities

Inner resistive layer Δ'

Growth rate of linear tearing mode

The helical field

Magnetic islands

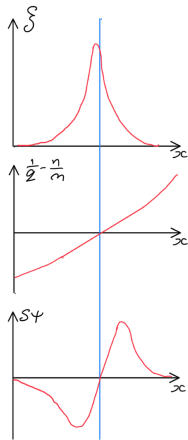
Tearing mode steady state island width

Neoclassical Tearing modes

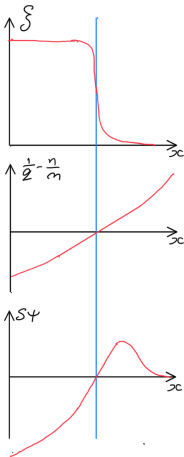
Driven tearing modes

Ideal Modes (basis of resistive instabilities)

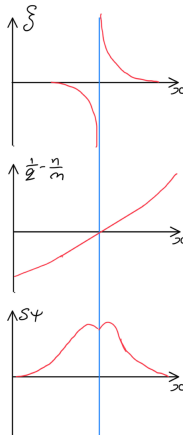
Ideal interchange mode



Ideal $m=1$ internal kink mode



Stable ideal mode (current sheet)



Ideal interchange modes and $m = 1$ internal kink modes are mostly driven by pressure gradients. Note that the flux $\delta\psi$, and hence the radial magnetic field, is zero on the rational surface, since from Eq. (3.31):

$$\delta B_0^r = \frac{imB_0}{R_0} \left(\frac{n}{m} - \frac{1}{q} \right) \xi_0^r$$

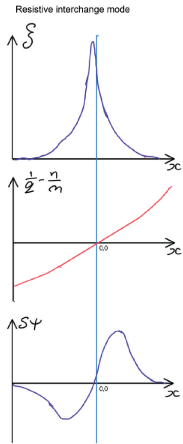
or the ideal limit of Eq. (4.23):

$$\delta\psi(r) = \frac{B_0 r}{R_0} \left(\frac{n}{m} - \frac{1}{q(r)} \right) \xi_0^r(r)$$

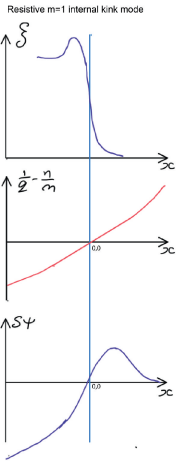
$$\delta\psi(x) \approx \frac{B_0 r_1}{R_0} \frac{n}{m} s_1 x \xi_0^r(x)$$

The ideal current sheet mode shown would be stable without resistivity. So, without resistivity, the mode isn't an instability. Since ξ_0^r is singular on the rational, the flux and radial field can be non-zero.

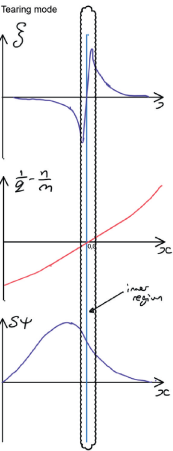
Resistive instabilities



Known as an even mode
Almost even in ξ^r
Almost odd in $\delta\psi$
Constant-psi doesn't apply
 $\delta\psi(x = 0) \neq 0$ (but small)
 $\delta\Delta' \sim 1$



$m = 1$ resistive kink is a special case.
Constant-psi doesn't apply
 $\delta\psi(x = 0) \neq 0$ (but small)
 $\delta\Delta' \sim 1$



Known as an odd mode
Almost odd in ξ^r
Constant-psi applies
 $\delta\psi(x = 0) \neq 0$ (large)
 $\delta\Delta' \sim \delta^2/r_s^2 \ll 1$

The resistive interchange mode is known as an even mode, or *twisting mode* because of the nearly evenness $\xi^r(x)$. The flux $\delta\psi(x)$ is nearly odd in x . Note $\delta\psi(x = 0)$ is non-zero (due to resistive correction in Eq. (4.23)), so there is some reconnection, but $\delta\psi(x = 0)$ is very small, and varies fast (changes sign) near x , so constant-psi approximation doesn't hold. Resistive $m = 1$ internal kink has some similar features to resistive interchange modes for equilibria stable to ideal $m = 1$.

The tearing mode is the resistive extension of the ideal current sheet mode. It can be unstable, i.e. it can be an instability, and it is primarily driven by current (so order ϵ^2 problem!). It is known as an odd mode, or *tearing mode* because of oddness of $\xi^r(x)$. Note $\delta\psi(x = 0)$ is large, and $\delta\psi(x)$ varies quite weakly with respect to x around $x = 0$, so the constant-psi approximation holds.

Resistive interchange in a torus are stable in circular tokamaks for $m/n > 1$ (see interchange modes later). We choose to investigate tearing modes in region of plasma where $q > 1$.

Inner resistive layer calculation

We can define Δ' in the layer directly from Eq.(4.23), noting that radial derivatives in $\delta\psi$ and ξ^r dominate derivatives with respect to the angular coordinates in the resonance region (e.g. $\nabla^2(\delta\psi/r) \approx r^{-1}\partial^2\delta\psi/\partial r^2$) so that Fourier analysing (keeping m harmonic only):

$$\frac{d^2\delta\psi}{dr^2} = \frac{\gamma}{\eta} \left[\delta\psi - \xi_0^r \frac{rB_0}{R_0} \left(\frac{n}{m} - \frac{1}{q(r)} \right) \right].$$

We now apply the constant-psi approximation (it is the only significant place it is used in this calculation). Applying Eq. (4.29), which states that $\delta\psi''/\delta\psi \ll (\xi_0^r)''/\xi_0^r$ we may replace $\delta\psi$ with $\delta\psi(r_s)$ on the RHS of the above equation, while allowing variation of ξ_0^r :

$$\frac{d^2\delta\psi(r)}{dr^2} = \frac{\gamma}{\eta} \left[\delta\psi(r_s) - \xi_0^r(r) \frac{rB_0}{R_0} \left(\frac{n}{m} - \frac{1}{q(r)} \right) \right] \quad (5.1)$$

where $q(r_s) = m/n$. We now expand around the rational surface so that

$$\frac{n}{m} - \frac{1}{q} \approx \frac{n}{m} s(r_s) x \quad \text{with} \quad x = \frac{r - r_s}{r_s} \quad \text{and} \quad s = \frac{r}{q} \frac{dq}{dr}.$$

Thus, changing the variable to x (so that $d^2\delta\psi/dr^2 = r_s^{-2}d^2\delta\psi/dx^2$), and integrating with respect to x in $-X \leq x \leq X$ we have clearly:

$$\left[\frac{\delta\psi'}{\delta\psi(r_s)} \right]_{-X}^X = \frac{1}{\delta\psi(r_s)} \left[\frac{1}{r_s} \frac{d\delta\psi}{dx} \right]_{-X}^X = \int_{-X}^X dx r_s \frac{\gamma}{\eta} \left[1 - \frac{\xi_0^r(x)}{\delta\psi(r_s)} \left(\frac{rB_0}{R_0} \right) \frac{n}{m} s(r_s) x \right], \quad (5.2)$$

which is Δ' in the layer in the limit $X \rightarrow \infty$ according to Eq. (4.28). It now remains to obtain $\xi_0^r(x)$ in the layer and this is done by solving Eq. (4.22) in the layer region, where, of course, inertia must be included (the LHS of Eq. (4.22)). We will be able to verify the asymptotic properties of the above as we increase X (exercises).

Inner resistive layer calculation

Due to the large radial derivatives in $\delta\psi$ and ξ_0^r in the inertial region, we keep only the terms in Eq. (4.22) with largest order derivatives. Keep also (for the moment) the $\delta\psi J_\phi$ term, and apply constant-psi approximation to that term. Therefore, in the layer we have,

$$\left(\frac{\gamma}{\omega_A}\right)^2 r^3 \frac{d^2 \xi_{r0}}{dr^2} = -m^2 \frac{R_0}{B_0} \left\{ r^2 \left(\frac{n}{m} - \frac{1}{q}\right) \frac{d^2 \delta\psi}{dr^2} + r\delta\psi(r_s) \frac{R_0}{B_0} \frac{dJ_\phi}{dr} \right\} \quad (5.3)$$

We now substitute Eq. (5.1) for $\delta\psi''$, and expand once again around the rational surface

$$\frac{d^2 \xi_0^r}{dx^2} = -\left(\frac{\gamma}{\omega_A}\right)^{-2} m^2 \frac{R_0}{r_s B_0} \left\{ \frac{n}{m} s(r_s) x \frac{r_s^2 \gamma}{\eta} \left[\delta\psi(r_s) - \xi_0^r \frac{r_s B_0}{R_0} \frac{n}{m} s(r_s) x \right] + \delta\psi(r_s) \frac{R_0}{B_0} \frac{dJ_\phi}{dx} \right\}$$

Now, let,

$$z = xd \quad \text{with} \quad d = \left(\frac{\omega_A^2 n^2 r_s^2 s^2}{\eta \gamma} \right)^{1/4}$$

to give

$$\left(\frac{d^2 \xi_0^r}{dz^2} - z^2 \xi_0^r \right) \left(\frac{d^2 B_0 \eta \gamma}{\omega_A^2 n m R_0 r_s s} \right) = -\frac{z \delta\psi(r_s)}{d} - \delta\psi(r_s) J'_\phi \frac{R_0 \eta}{B_0 \gamma r_s^2}.$$

This equation is written in terms of normalised variable $y(z)$:

$$\frac{d^2 y(z)}{dz^2} - z^2 y(z) = -z - J'_\phi \frac{R_0 \eta d}{B_0 \gamma r_s^2} \quad \text{with} \quad y(z) = \frac{r_s B_0}{R_0} \frac{ns}{md} \left(\frac{\xi_0^r(z)}{\delta\psi(r_s)} \right). \quad (5.4)$$

The inhomogeneity on the RHS of the differential equation comprises the sum of odd and even contributions in z . As a consequence, the solution $y(z)$ comprises the corresponding sum in odd and even contributions in z . It is clear that the even component of $y(z)$ vanishes in the integral of Eq. (5.2), when integrated with respect to z across the rational surface, so for this reason, we are permitted to drop the even term proportional to J'_ϕ , and thus we solve

$$\frac{d^2 y}{dz^2} = -z(1 - zy).$$

Inner resistive layer calculation

Equation (5.2) can be written in terms of y and z as follows:

$$\frac{\delta\psi'}{\delta\psi(r_s)} \Big|_{-X}^X = \frac{\gamma\tau_R}{dr_s} \int_{-X}^X dz(1 - yz) \quad \text{where} \quad \tau_R = \frac{r_s^2}{\eta}.$$

Moreover, it is convenient to define d in terms of the ratio of the resistive time and the Alfvén time:

$$S = \frac{\tau_R}{\tau_A} \equiv \tau_R \omega_A \quad \text{which is the Lundquist number, } S \sim 10^8 \text{ or larger in large tokamaks}$$

Giving $d^4 = n^2 s^2 S \omega_A / \gamma$. It can be shown that a measure of the **layer width** δ normalised to the singular radius r_s is

$$\frac{\delta}{r_s} = \frac{1}{d} = \left[\frac{\gamma}{\omega_A n^2 s^2 S} \right]^{1/4}. \quad (5.5)$$

It will be verified in the exercises that δ is indeed the layer width by showing that $y(z)$ agrees with the ideal inertialess expectation for $y(z) \sim 1/z$ for $|z| = |r - r_s|/\delta > 1$, but for $|z| < 1$ the effect of resistivity (tearing) on y will be evident.

From $d^2 y/dz^2 = -z(1 - zy)$ it is seen that

$$\frac{\delta\psi'}{\delta\psi} \Big|_{-X}^X = \frac{\gamma\tau_R}{dr_s} \int_{-X}^X dz(1 - yz) = -\frac{\gamma\tau_R}{dr_s} \int_{-X}^X dz \frac{1}{z} \frac{d^2 y}{dz^2}.$$

Integrating by parts, and noting that the boundary term is zero because the dy/dz is even in z , yields

$$\frac{\delta\psi'}{\delta\psi} \Big|_{-X}^X = -\frac{\gamma\tau_R}{dr_s} \int_{-X}^X dz \frac{1}{z^2} \frac{dy}{dz}. \quad (5.6)$$

Inner resistive layer calculation

Rutherford and Furth, 1971, showed that

$$y = \frac{z}{2} \int_0^1 d\mu \frac{\exp(-z^2 \mu/2)}{(1 - \mu^2)^{1/4}} \quad (5.7)$$

is the odd solution of Eq. (5.4), i.e. it is a solution of

$$\frac{d^2 y}{dz^2} = -z(1 - zy)$$

which can easily be verified by substitution. Differentiating Eq. (5.7), we have

$$\frac{dy}{dz} = \frac{1}{2} \int_0^1 d\mu (1 - \mu z^2) \frac{\exp(-z^2 \mu/2)}{(1 - \mu^2)^{1/4}}.$$

and substituting this into Eq. (5.6) yields,

$$\frac{\delta \psi'}{\delta \psi} \Big|_{-X}^X = -\frac{\gamma \tau_R}{dr_s} \int_{-X}^X dz \int_0^1 d\mu \frac{(1 - \mu z^2)}{2z^2} \frac{\exp(-z^2 \mu/2)}{(1 - \mu^2)^{1/4}}. \quad (5.8)$$

The exercises will show that the above saturates with increasing X when X is about 5, i.e. within a few layer widths. It is also shown that the layer width is very small, so that matching with the outer region is reliable. In particular, it will be shown that $\delta \Delta' \ll 1$ which is required for the constant-psi approximation. Hence it is safe to take $X \rightarrow \infty$ for the above integration limits. Changing the order of integration we have from Eqs. (4.28) and (5.8):

$$\Delta' = -\gamma \tau_R \frac{\delta}{r_s} \int_0^1 \frac{d\mu}{2(1 - \mu^2)^{1/4}} \int_{-\infty}^{\infty} dz \left(\frac{1}{z^2} - \mu \right) \exp(-z^2 \mu/2).$$

The inner integral is just $-2\sqrt{2\pi\mu}$. Hence,

$$\Delta' = \gamma \tau_R \frac{\delta}{r_s} \int_0^1 d\mu \frac{(2\pi\mu)^{1/2}}{(1 - \mu^2)^{1/4}} = \gamma \tau_R \frac{\delta}{r_s} \left(\frac{2\pi \Gamma(3/4)}{\Gamma(1/4)} \right)$$

Growth rate of linear tearing mode

On substituting the definition of δ and using also the definition of S , we have the inner Δ' as defined by Eq. (4.28):

$$\Delta' = \left(\frac{2\pi\Gamma(3/4)}{\Gamma(1/4)} \right) \frac{(\gamma/\omega_A)^{5/4} S^{3/4}}{r_s(ns)^{1/2}}, \quad \text{with} \quad \frac{2\pi\Gamma(3/4)}{\Gamma(1/4)} \approx 2.12. \quad (5.9)$$

Now for the crucial part. The asymptotes at $z \rightarrow \pm\infty$ for logarithmic derivatives of $\delta\psi$ in the layer are matched with the asymptotes of the logarithmic derivatives of $\delta\psi(\text{ideal})$ in the outer region, as defined by Eq. (4.30), which is

$$\Delta' = \lim_{\delta r \rightarrow 0} \frac{\delta\psi(\text{ideal})'}{\delta\psi(\text{ideal})} \Big|_{r_s - \delta r}^{r_s + \delta r}$$

One can then obtain the growth rate by solving Eq. (4.24) for $\delta\psi$ in the ideal region, calculating the logarithmic derivatives on each side of r_s , and substituting into Δ' . Matching this outer Δ' with the inner Δ' of Eq. (5.9), i.e. $\Delta' = \Delta'$ and rearranging for the growth rate, we have

$$\frac{\gamma}{\omega_A} = \left[\frac{\Gamma(1/4)r_s\Delta'}{2\pi\Gamma(3/4)} \right]^{4/5} S^{-3/5} (ns)^{2/5}. \quad (5.10)$$

Thus, instability requires that $\Delta' > 0$, and this condition in turn is governed by the global current profile. For the case shown in the figure on slide 99, we have $r_s\Delta' = 4.25058$, i.e. the mode is unstable. Taking $S = 10^8$, this gives $\gamma/\omega_A \sim 10^{-5}$, which is a slow growth rate compared to ideal growth rates (typically $\gamma/\omega_A \sim 10^{-2} - 10^{-3}$).

There are very important non-linear extensions to this description of linear tearing instabilities. As will be seen, Δ' remains a fundamental parameter for non-linear tearing modes. Non-linear tearing modes are often manifested experimentally as neoclassical tearing modes (NTMs). These modes are at saturated amplitude (not growing), the amplitude elevated by bootstrap current.

The helical field

Consider the parallel wave-number ($k_{\parallel} = -i\mathbf{b} \cdot \nabla$, see exercises)

$$k_{\parallel} = \frac{1}{q(r)R_0} (nq(r) - m)$$

We know that a rational surface occurs where $k_{\parallel} = 0$, i.e. at the location

$$q(r_s) \equiv q_s = m/n.$$

We assume that the perturbations have the usual angular dependence $\sim \exp(im\chi)$ where

$$\chi = \frac{n}{m}\phi - \theta = \frac{1}{q_s}\phi - \theta.$$

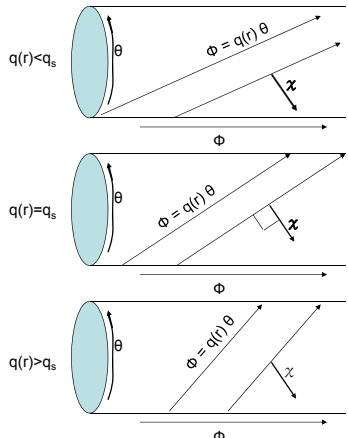
It turns out that the coordinate χ is orthogonal to the magnetic field lines on the rational surface, and near orthogonal close to the rational.

Interpretation is made easier by assuming straight field line coordinates for which $q(r) = d\phi/d\theta$ so that a field line is described by

$$\phi = q\theta \quad (+ \text{ constant})$$

This can be compared with the χ coordinate in ϕ - θ space, which is **constant** for

$$\phi = q_s\theta \quad (+ \text{ constant})$$



The helical field

Our goal now is to consider the helical field $B^X = r\mathbf{B} \cdot \nabla\chi$, and the helical flux Ψ linking this helical field, i.e. $B^X = \partial\Psi/\partial r$ (note that a true flux would have an extra factor R_0). For a description of magnetic islands we need to clearly distinguish the equilibrium field (and flux) from the total field (and flux). So, we use notation:

$$\mathbf{B} = \mathbf{B}_0 + \mathbf{B}_1, \quad B^X = B_0^X + B_1^X, \quad \Psi = \Psi_0 + \Psi_1.$$

Keep in mind that magnetic field lines lie on surfaces of constant flux, including on this helical total flux $\Psi = \Psi_0 + \Psi_1$

Consider now **perturbed fields** in these coordinates. Since $\nabla \cdot \mathbf{B}_1 = 0$, and since perturbed $B_{1,\parallel}$ is small (it is a finite beta effect - see exercises), and since $\partial/\partial l \propto k_{\parallel}$ (again small) then:

$$\nabla \cdot \mathbf{B}_{1,\perp} \approx \frac{1}{r} \frac{\partial}{\partial r} (r B_1^r) + \frac{1}{r} \frac{\partial B_1^X}{\partial \chi} \approx 0$$

Thus, in terms of a flux variable Ψ we have:

$$B_1^r = -\frac{1}{r} \frac{\partial \Psi_1}{\partial \chi} \quad \text{and} \quad B_1^X = \frac{\partial \Psi_1}{\partial r} \quad (5.11)$$

So that we can plot field line surfaces and island structures, we adopt real variables. Choose B_1^r to be odd in χ (so that Ψ even in χ). Hence, since $n\phi - m\theta = m\chi$ then $B_1^r = \hat{B}_1^r \sin(m\chi)$ and

$$\Psi_1 = \frac{r}{m} \hat{B}_1^r \cos(m\chi). \quad (5.12)$$

The helical field

Consider now the **equilibrium helical flux** Ψ_0 associated with the helical equilibrium field B_0^χ . We first note that the equilibrium field $B_0 = F(\psi)\nabla\phi + \nabla\phi \times \nabla\psi$ can equivalently be written in Clebsch form:

$$B_0 = \nabla\beta \times \nabla\psi_0, \quad \text{with} \quad \beta = \phi - q\theta.$$

Hence the contravariant helical equilibrium field written in terms of θ and ϕ is

$$B_0^\chi = rB_0 \cdot \nabla\chi = r\nabla(\phi - q\theta) \times \nabla(\phi/q_s - \theta) \cdot \nabla\psi_0 = r \left(\frac{q(r)}{q_s} - 1 \right) \nabla\theta \times \nabla\phi \cdot \nabla\psi_0.$$

Meanwhile the contravariant covariant equilibrium poloidal field is

$$B_0^\theta = r\vec{B} \cdot \nabla\theta = r\nabla\phi \times \nabla\psi_0 \cdot \nabla\theta.$$

Hence,

$$B_0^\chi = B_0^\theta \left(\frac{q(r)}{q_s} - 1 \right) \approx B^\theta(r_s)s(r_s)x,$$

where we recognise the ‘layer’ variable, $x = (r - r_s)/r_s$ and the magnetic shear s . The equilibrium helical flux Ψ_0 , from the definition $B^\chi = \partial\Psi/\partial r = r_s^{-1}\partial\Psi/\partial x$, which applies to perturbed and equilibrium quantities near the rational surface, is:

$$\Psi_0 = r_s \int dx B_0^\chi = \int dx B_0^\theta(r_s)s(r_s)x = \frac{1}{2}B_0^\theta s(r_s)r_s x^2$$

where we note that B_0^θ otherwise depends on x through higher order (in ϵ) correction $\sim 1/R$.

Magnetic islands

We therefore have the total helical flux:

$$\Psi = \Psi_0(x) + \Psi_1(x, \chi, t) \quad \text{with} \quad \Psi_0 = \frac{1}{2} B_0^\theta(r_s) r_s s x^2, \quad \Psi_1 = \frac{r}{m} \hat{B}_1^r(x, t) \cos(m\chi).$$

Recall that field lines lie on flux surfaces. To solve for the trajectory on the field line in coordinates (x, χ) we thus consider the total flux Ψ a constant. Hence, we obtain the **field line trajectory** assuming weak variation of Ψ_1 in x (constant-psi):

$$x^2 = \frac{2}{r_s s B_0^\theta} \left[\Psi - \frac{r_s \hat{B}_1^r(t)}{m} \cos(m\chi) \right], \quad (5.13)$$

all (on the RHS) evaluated at r_s . This marks out the island structure. Sufficiently far from the rational, specifically for $\Psi > r_s \hat{B}_1^r/m$ we have wobbling unbroken field lines (ideal MHD).

Close to the rational surface, for which $\Psi < r_s \hat{B}_1^r/m$ the field lines are broken, to reveal island loops.

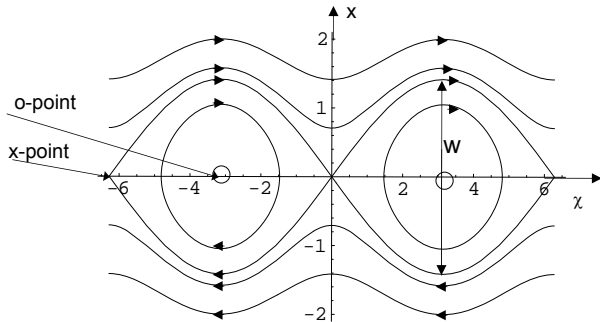
For $\Psi = r_s \hat{B}_1^r/m$ we are on the separatrix of the island. Thus the full island width (see exercises) is

$$w(t) = 4r_s \left(\frac{\hat{B}_1^r(t)}{ms B_0^\theta} \right)^{1/2}. \quad (5.14)$$

We see that the island is larger for small poloidal field, and reduced magnetic shear (again small shear invokes weakness in the plasma configuration - this time for resistive MHD instabilities. Although small shear reduces growth rates too).

Also small m leads to larger magnetic islands. It is generally found that modes with small mode numbers are the most degrading (poor transport properties due to rapid parallel motion ‘across’ island structure).

Magnetic islands

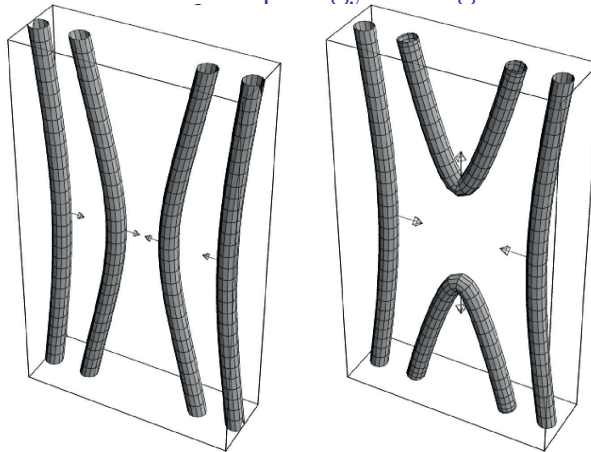


Magnetic island chain assuming poloidal mode number $m=1$

The lines indicate field line trajectories in the (x, χ) coordinates, and on each line the total Ψ is constant.

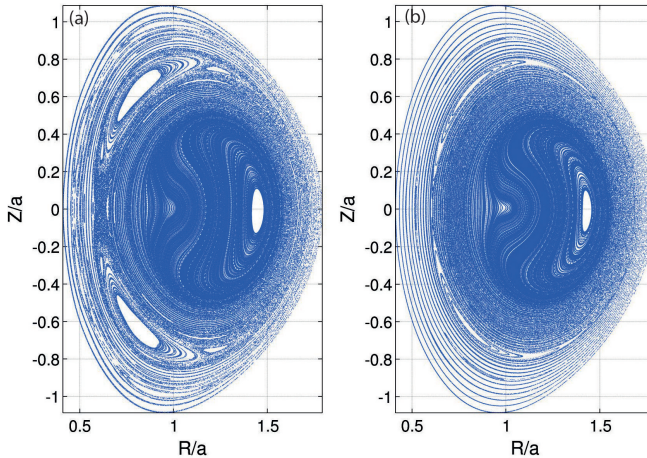
Since the equilibrium radial field is zero, each of the lines above has non-zero B_1^r . Thus, it is seen the $B_1^r \neq 0$ even at the equilibrium rational surface. This topological change is possible only under the resistive MHD model. Realistic ideal MHD instabilities have $B_1^r(x = 0) = 0$, but it isn't necessarily zero under resistive MHD:

$$\delta B_0^r(\text{ideal}) = \frac{imB_0}{R_0} \left(\frac{n}{m} - \frac{1}{q} \right) \xi_0^r \quad \text{and} \quad \delta B_0^r(\text{res}) = \frac{imB_0}{R_0} \left(\frac{n}{m} - \frac{1}{q} \right) \xi_0^r - \frac{\eta}{\gamma} \nabla^2 \delta B_0^r(\text{res})$$



Resistivity allows field lines to slip through the fluid, allowing new field line topology to be created with time. This would not be possible if the field lines were frozen into the fluid (as for ideal MHD). The sketch here indicates clearly how a magnetic island might develop in the laboratory plasma. Consider the horizontal direction to be radial direction in tokamak plasma, and the reconnection takes place on the vertical line where the rational flux surface lies. The new topology requires a finite magnetic field on this surface which points in the horizontal direction, that is a radial perturbed field on the rational, which is only allowed in the resistive MHD model. Without resistivity we will just have wobbling field lines with the wobble in the radial direction vanishing as we approach the rational surface.

Magnetic islands



XTOR island. (a) with bootstrap, (b) w/o bootstrap. Kleiner, Graves, Ph.D. thesis (EPFL)

XTOR initial value code solved the resistive MHD equations nonlinearly. Poincaré plots over the poloidal cross section enables us to see constant Ψ surfaces. The core mode is in fact a non-resonant internal kink mode (no island). The large outer island is an $n = 1, m = 2$ mode associated with $q_s = 2$. Other shorter wavelength modes are visible too. Note in this plot χ is mapped out in θ (since we plot on constant ϕ), and the x variable would be $x = (r - r_s)/r_s$, with r_s taken to be the minor radius at the island o-point or x-point.

Non-linear tearing modes

Notice that the XTOR islands shown were non-linearly saturated, meaning that they were not growing. We do not yet have an evolution equation for the non-linear stage of the island development.

In the following non-linear treatment we do not assume linear growth, i.e. \mathbf{B}_1 **does not** grow as $\exp(\gamma t)$, so explicit time derivatives are retained in the equations. Begin with Faraday's law

$$\frac{\partial \mathbf{B}_1}{\partial t} = -\nabla \times \mathbf{E}_1$$

now substitute Ohms law $\mathbf{E}_1 + \mathbf{u}_1 \times \mathbf{B}_0 = \eta \mathbf{j}_{1,\text{Ohm}}$:

$$\frac{\partial \mathbf{B}_1}{\partial t} = -\nabla \times (\eta \mathbf{j}_{1,\text{Ohm}} - \mathbf{u}_1 \times \mathbf{B}_0),$$

where $\mathbf{j}_{1,\text{Ohm}}$ is the perturbed MHD Ohmic current. Finally we employ Ampère's law $\nabla \times \mathbf{B}_1 = \mathbf{j}_1$, but we write the total current as the sum of Ohmic (MHD) current and perturbed currents associated with external sources (or non-Ohmic currents), e.g. from cyclotron heating or the bootstrap current. So substituting

$\mathbf{j}_{1,\text{Ohm}} = \mathbf{j}_1 - \mathbf{j}_{1,\text{non-Ohm}} = \nabla \times \mathbf{B}_1 - \mathbf{j}_{1,\text{non-Ohm}}$ we have:

$$\frac{\partial \mathbf{B}_1}{\partial t} = -\nabla \times \left[\eta \left(\nabla \times \mathbf{B}_1 - \mathbf{j}_{1,\text{non-Ohm}} \right) - \mathbf{u}_1 \times \mathbf{B}_0 \right]. \quad (5.15)$$

Now a key simplification - **we ignore the inertia associated with the convective term involving the fluid velocity \mathbf{u}_1** . The plasma inertia, and associated displacement $\xi^r = \gamma^{-1} u_1^r$ was crucial for establishing the linear resistive problem in the layer. But, in the non-linear regime, the plasma inertia contribution is weak compared to that of the diffusion of the magnetic field. Again assuming large radial derivatives we have on taking the radial component of Eq. (5.15):

$$\frac{\partial B_1^r}{\partial t} = \eta \frac{\partial^2 B_1^r}{\partial r^2} - \nabla r \cdot \nabla \times \left[\eta \mathbf{j}_{1,\text{non-Ohm}} \right]. \quad (5.16)$$

Essential non-linear tearing modes

First let us consider the essential case where there is no current from external sources. So, taking Eq. (5.16) with $j_{1,\text{non-Ohm}} = 0$ and using $\Psi_1 = -irB_1^r/m$ assuming strong radial derivatives in B_1^r we have,

$$\frac{\partial \Psi_1}{\partial t} = \eta \frac{\partial^2 \Psi_1}{\partial r^2}. \quad (5.17)$$

Integrating in radius across the island (assuming η varies weakly) we have

$$\int_{r_s - w/2}^{r_s + w/2} dr \frac{\partial \Psi_1}{\partial t} = \eta(r_s) \frac{\partial \Psi_1}{\partial r} \Big|_{r_s - w/2}^{r_s + w/2}$$

In order to make some analytic progress we assume that the radial variation of Ψ_1 is weak over w . This is of course the constant-psi approximation:

$$w \frac{d\Psi_1(r_s)}{dt} = \eta(r_s) \frac{\partial \Psi_1}{\partial r} \Big|_{r_s - w/2}^{r_s + w/2}.$$

We now use the result from the linear derivation of the island width w . In particular, from Eq. (5.14) we can make a relation between the time evolution of $\Psi_1(t)$ and $w(t)$:

$$\Psi_1(r_s, t) = Cw(t)^2$$

where C is a constant. This easily yields (exercises)

$$\frac{dw}{dt} = \frac{\eta(r_s)}{2} \frac{1}{\Psi_1} \frac{d\Psi_1}{dr} \Big|_{r_s - w/2}^{r_s + w/2}.$$

The right hand side is the Δ' in the layer, but it is dependent on w , i.e. it is essentially Δ'_δ in Eq. (7.19) with $\delta = w/2$. We then obtain the **Rutherford equation**

$$\frac{dw}{dt} = \frac{\eta(r_s)}{2} \Delta'(w) \quad \text{with} \quad \Delta'(w) = \frac{1}{\Psi_1} \frac{d\Psi_1}{dr} \Big|_{r_s - w/2}^{r_s + w/2}.$$

Essential non-linear tearing modes

In this non-linear treatment we match at the island width instead of matching the asymptotes (which is what we did for the linear treatment).

Hence Δ' in the layer must be matched with Δ' in the ideal MHD external region evaluated at periphery of the island. Hence we obtain,

$$\Delta'(w) = \frac{1}{\Psi_1} \frac{d\Psi_1}{dr} \Big|_{r_s-w/2}^{r_s+w/2}$$

from calculating the $\Psi_1(r)$ via solving Eq. (4.24) (noting $\delta\psi \equiv \Psi_1$), i.e.

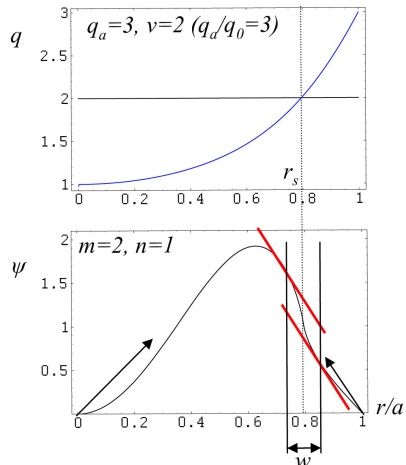
$$r \frac{d}{dr} \left(r \frac{d\Psi_1}{dr} \right) + \left(\frac{R_0}{B_0} \right) \frac{r q m \Psi_1}{n q - m} \frac{dJ_\phi}{dr} - m^2 \Psi_1 = 0.$$

Hence the evolution equation for $w(t)$ is

$$\frac{dw}{dt} = \frac{\eta}{2} \Delta'(w) \quad \text{with} \quad \Delta'(w) = \frac{1}{\Psi_1} \frac{d\Psi_1}{dr} \Big|_{r_s-w/2}^{r_s+w/2}.$$

A saturated island occurs for:

$$dw/dt = 0, \text{ and this in turn requires } \Delta'(w) = 0.$$

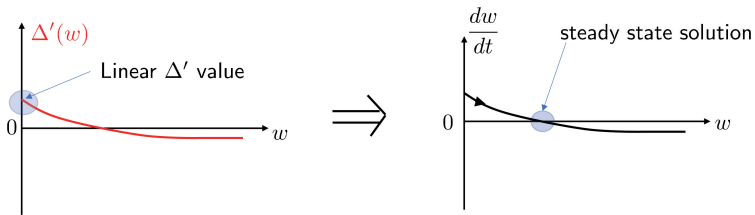


Tearing mode steady state island width

Figure shows the evolution of $w(t)$ according to:

$$\frac{dw}{dt} = \frac{\eta}{2} \Delta'(w)$$

where $\Delta' > 0$ during the linear phase. The mode amplitude saturates because the external solution exhibits the property $\Delta'(w) = 0$ for sufficiently large w .

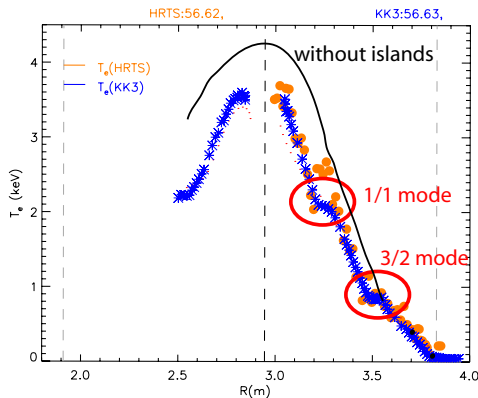


From the solution to $w(t)$ and the mode number we can obtain $B_1^r(t)$ via Eq. (5.14). Knowledge of m and equilibrium reconstruction is also required (for poloidal equilibrium field, and magnetic shear).

Neoclassical Tearing modes

JET pulse 80869 exhibits local flattening of the temperature profile due to the presence of magnetic islands.

- ▶ The width of the flat regions corresponds approximately to the island width (degree of flattening in fact depends on helical angle, see details next). So, the ECE diagnostic provides a useful measurement of island location and the helically averaged island width (potentially in real time).
- ▶ Temperature and density gradients cannot be sustained across the island because heat and particles travel rapidly along the magnetic field lines (parallel transport). Consider the field line trajectory in $x - \chi$ coordinates.
- ▶ This local flattening of the pressure profile ($P(r) = n(r)T(r)$) locally nullifies the equilibrium bootstrap current. We will see that this affect destabilises tearing modes. The effect can be included in the evolution equation for w , and it is seen that we obtain larger islands. These are called neoclassical tearing modes (NTMs).



Neoclassical Tearing modes

The bootstrap current is derived from neoclassical transport. Hence it is due to toroidicity (trapped particles) and it depends on collisionality regime. Here we set,

$$\mathbf{j}_{BS} \approx j_{BS} \mathbf{e}_\phi, \quad \text{with} \quad j_{BS} = -\frac{dP}{dr} \frac{\epsilon^{1/2}}{B_0^\theta}.$$

This is the bootstrap current that we would expect before the onset of a tearing mode, i.e. at the initial equilibrium:

$$\mathbf{j}_{0,non-Ohm} = \mathbf{j}_{BS},$$

But, the transport of particles and heat along the closed field lines (closed in $x - \chi$) forces the pressure inside the islands to vanish. Hence the bootstrap current will vanish locally too.

Mathematically therefore there exists a **perturbed current that cancels the initial equilibrium bootstrap current within the island**. This current of course depends on the angle χ (local island width fluctuates). At the rational surface:

$$\mathbf{j}_{1,non-Ohm} \equiv \hat{\mathbf{j}}_{1,non-Ohm} \cos(m\chi) = -j_{BS} \cos(m\chi) \mathbf{e}_\phi$$

The **perturbed** evolution equation for the radial component of perturbed magnetic field, including non-Ohmic current is Eq. (5.16). Using as before $B_1^r = \hat{B}_1^r \sin(m\chi)$ we have

$$\sin(m\chi) \frac{\partial \hat{B}_1^r}{\partial t} = \eta \left(\frac{\partial^2 \hat{B}_1^r}{\partial r^2} \sin(m\chi) + [\nabla \times (j_{1,non-Ohm} \mathbf{e}_\phi)] \cdot \mathbf{e}_r \right)$$

Use: $[\nabla \times (j_{1,non-Ohm} \mathbf{e}_\phi)] \cdot \mathbf{e}_r \approx -(m/r) \mathbf{e}_\phi \cdot \hat{\mathbf{j}}_{1,non-Ohm} \sin(m\chi) = (m/r) j_{BS} \sin(m\chi)$ to finally give (using $\Psi_1 \propto r \hat{B}_1^r$) an evolution equation for the perturbed helical flux:

$$\frac{\partial \Psi_1}{\partial t} = \eta \left[\frac{\partial^2 \Psi_1}{\partial r^2} + j_{BS} \right] \quad (5.18)$$

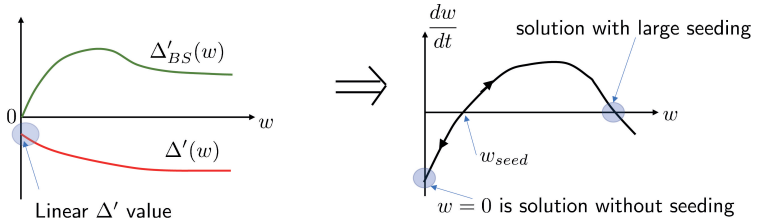
Neoclassical Tearing modes and seeding

The exercises lay out the procedure for obtaining the following modified-Rutherford-equation. Here we include the effect of bootstrap, but for simplicity neglect other effects known in the literature (e.g. GGJ high pressure corrections, polarisation current etc):

$$\frac{dw}{dt} = \frac{\eta(r_s)}{2} \left(\Delta'(w) + \Delta'_{BS}(w) \right), \quad \Delta'_{BS}(w) = j_{BS}(r_s) \frac{16r_s}{sB_0^\theta w} = - \frac{dP}{dr} \frac{16\epsilon^{1/2}r}{s(B_0^\theta)^2 w} \Big|_{r_s}.$$

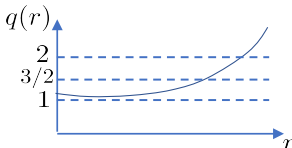
Notice that $\Delta'_{BS}(w)$ is positive (hence destabilising) for all w if $P' < 0$. The non-linear derivation isn't valid in the limit $w \rightarrow 0$ where Δ'_{BS} diverges (recall neglect of inertia etc). In the literature, $\Delta'_{BS}(w)$ is killed in the following ad-hoc way for small w via a constant w_c . We may add effect of toroidal current drive $j_{cd} = j_{cd} \mathbf{e}_\phi$, stabilising if $j_{cd}(r_s) < 0$, destabilising if $j_{cd}(r_s) > 0$ (realtime NTM control experiments exploit this if island position can be tracked):

$$\frac{dw}{dt} = \frac{\eta(r_s)}{2} \left(\Delta'(w) + \Delta'_{BS}(w) + \Delta'_{cd}(w) \right), \quad \text{with} \quad \Delta'_X(w) = j_X \frac{16r}{sB_0^\theta} \left(\frac{w}{w_c^2 + w^2} \right) \Big|_{r_s}.$$

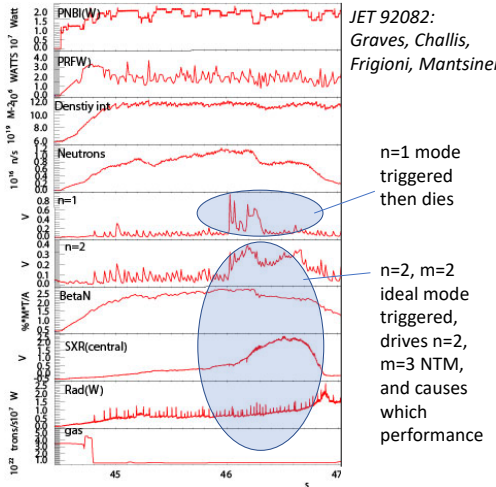


This is known as the **modified Rutherford equation**. Tokamak equilibrium are usually designed with q -profiles such that $\Delta'(0) < 0$ (ideal stable). The destabilising effect of bootstrap requires, according to this equation, a seed island for establishing an NTM (e.g. from a sawtooth crash).

Driven tearing modes

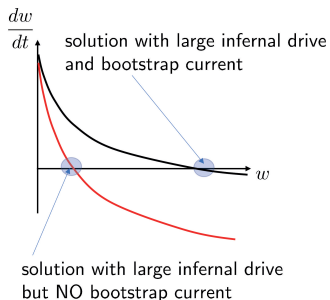
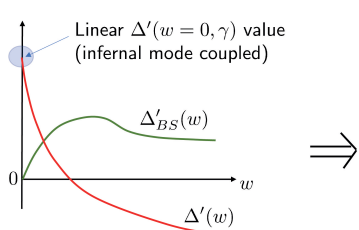


- JET Hybrid DT preparation
- Sawteeth avoided. High performance
- Non-resonant $n=2, m=2$ LLM drives $n=2, m=3$ tearing mode
- These modes are intolerable in JET because they enhance tungsten accumulation. Different from e.g. DIII-D which builds scenarios based on saturated tearing modes
- Tearing mode grows to large amplitude over 1ms. Much faster than standard resistive timescales



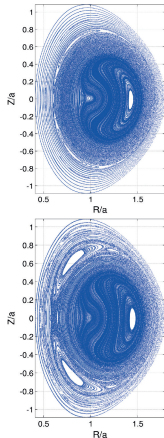
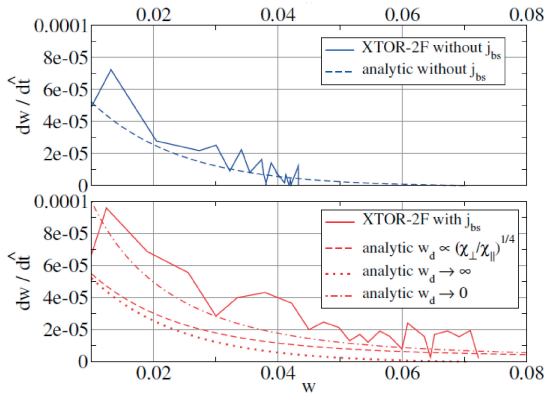
Driven tearing modes

$$\frac{dw}{dt} = \Delta'(w, \gamma) + \Delta'_{BS}(w)$$



In addition to seeding there are other processes for creating tearing modes. Such as toroidal coupling with other MHD modes that can drive tearing modes linearly, forcing linear $\Delta' > 0$. This route can establish NTMs during non-linear stage as well [Kleiner, Graves, EPFL thesis].

Driven tearing modes



These simulations show that the non-linear XTOR code confirms that saturated tearing modes and NTMs can be driven by toroidal coupling with infernal modes. The code recovers the driven Rutherford equations proposed. There are many important physics processes that could be taken into account in future work such as shear flows.